Electronic Supplementary Material (ESI) for Journal of Materials Chemistry A.

Electronic Supplementary Information

PtRu nanocubes as bifunctional electrocatalysts for ammonia electrolysis

Qi Xue,[‡a] Yue Zhao,[‡a] Jingyi Zhu,[a] Yu Ding,[a] Tiaojiao Wang,[a] Huiying Sun,[a] Fumin Li,[*a] Pei Chen,[a] Pujun Jin,[a] Shibin Yin,[b] and Yu Chen[*a]

[a] Key Laboratory of Macromolecular Science of Shaanxi Province, Key Laboratory of Applied Surface and Colloid Chemistry (MOE), Shaanxi Key Laboratory for Advanced Energy Devices, School of Materials Science and Engineering, Shaanxi Normal University, Xi'an 710062, PR China.

[b] MOE Key Laboratory of New Processing Technology for Non-ferrous Metals and Materials, Guangxi Key Laboratory of Processing for Non-ferrous Metals and Featured Materials, Guangxi University, Nanning, Guangxi 530004, PR China

[‡]These authors contributed equally to this work.

* Corresponding authors:

E-mail: ndchenyu@gmail.com (Y. Chen); ifuminxs@gmail.com (F. M. Li)

DFT calculation: Material studio within the local density approximation (LDA) was used to execute the DFT calculation of Pt_6Ru-NCs and Pt-NCs. The plane-wave energy cut off was 400 eV with norm-conserving pseudopotentials. The Brillouin zone was inside a 2 × 2 × 2 Monkhorst-Pack grid. The structure was totally optimized until the force on each atom is less than 10^{-3} eV/Å. The height of vacuum layer was set as 25 Å. The free energy (G) was computed based on G = E + ZPE - TΔS. Total energy was expressed by E. The zero-point energy was expressed by ZPE. The entropy (ΔS) of each adsorbed state were yielded from DFT calculation, and applied potential was expressed by ΔU. The thermodynamic corrections for gas molecules were from standard tables.

Figures

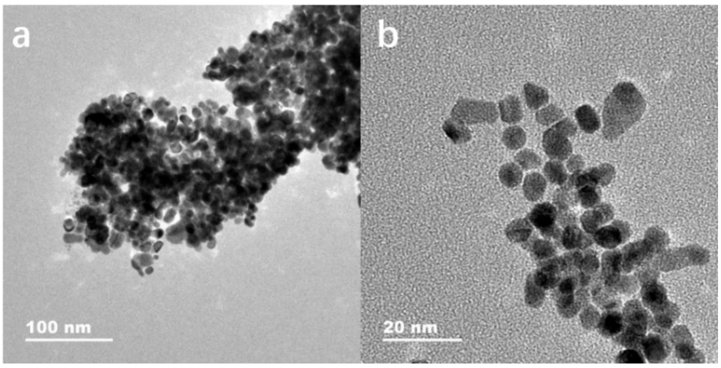

Fig. S1 TEM images of Pt_6Ru-NCs without (a) PAH or (b) HCHO.

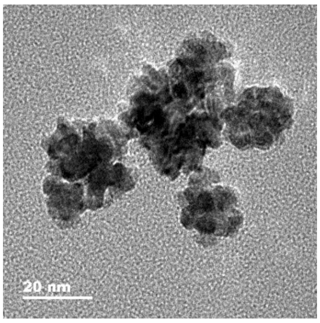

Fig. S2 TEM image of Ru nanoparticles.

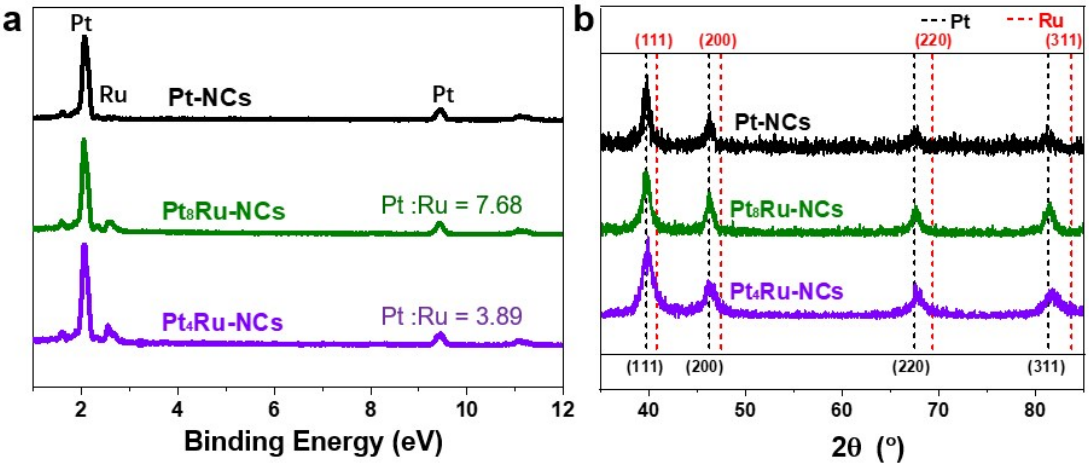

Fig. S3 (a) EDX spectrum, (b) XRD pattern of Pt-NCs and Pt_xRu-NCs.

Pt_xRu-NCs with different Pt/Ru mole ratio can be easily synthesized by changing the feed amount of $RuCl_3$. EDX spectra provide a convincing basis for the formation of Pt_xRu-NCs with different Pt/Ru mole ratios, which are consistent with their feed ratios (Fig. S3a). XRD patterns exhibit that the characteristic diffraction peaks of Pt in Pt_xRu-NCs shift positively with increasing Ru (Fig. S3b). The diffraction peaks of the (111) plane of Pt_8Ru-NCs and Pt_4Ru-NCs are located at 2θ angles of 39.83° and 39.96°, respectively. According to Vegard's law, the Pt content of Pt_8Ru-NC and Pt_4Ru-NC are 88.95% and 80.15%, respectively. Further indicate that more Ru are alloyed with Pt. TEM images show that both Pt-NCs, Pt_8Ru-NCs and Pt_4Ru-NCs are well-defined nanocubes. HR-TEM images reveal that Pt-NCs (Fig. S4a), Pt_8Ru-NCs (Fig. S4b) and Pt_4Ru-NCs (Fig. S4c) are highly crystalline with exposed (100) plane; the lattice plane show interplanar distances of 0.196 nm, 0.195 nm and 0.193 nm, respectively.

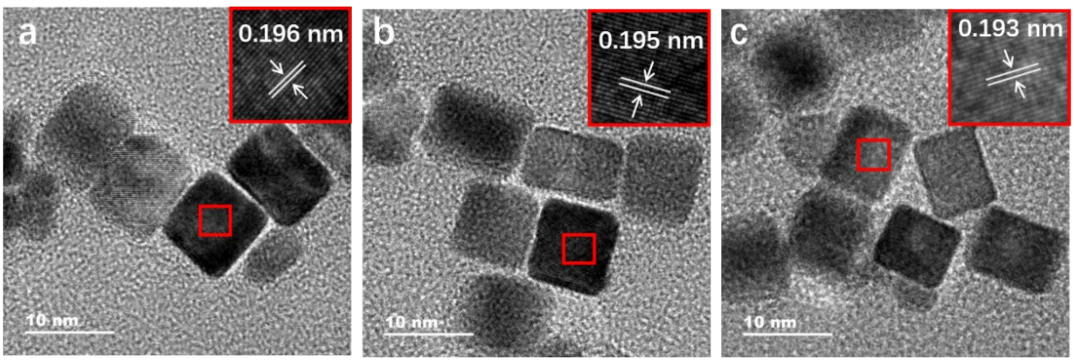

Fig. S4 TEM images of (a) Pt-NCs and (b) Pt_8Ru-NCs and b) Pt_4Ru-NCs.

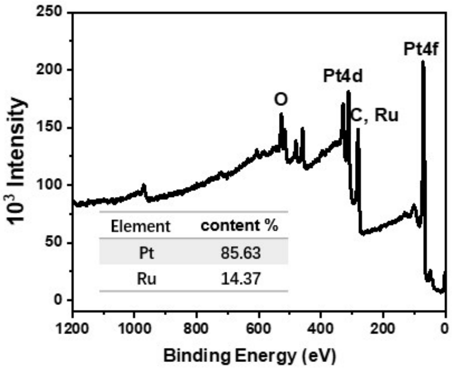

Fig. S5 XPS images of Pt_6Ru-NCs.

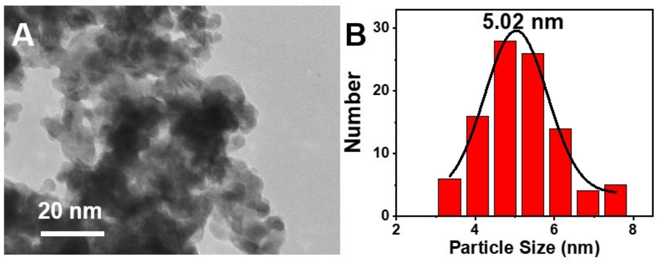

Fig. S6 TEM image and corresponding particle size distribution histogram of Pt-cNCs.

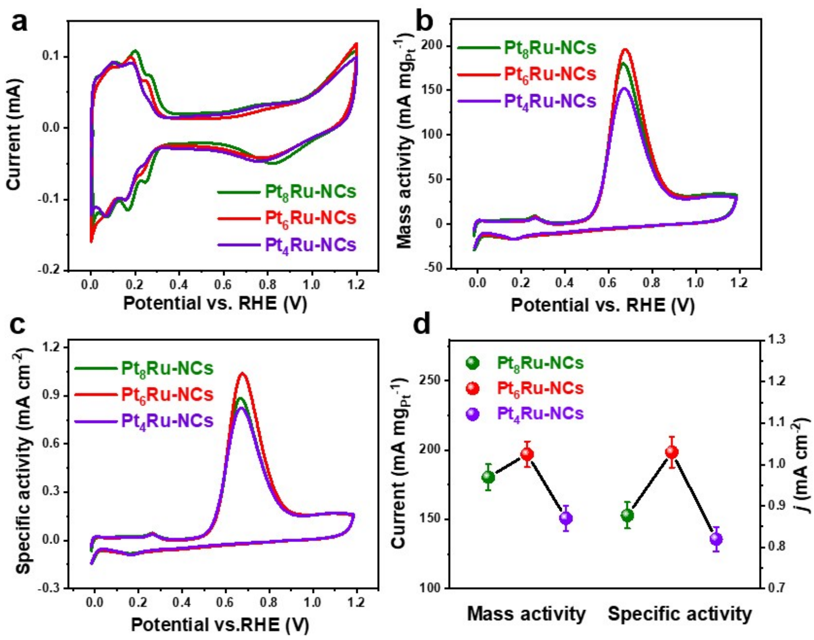

Fig. S7 (a) CV curves of various Pt_xRu-NCs in 1M $HClO_4$ solution at 50 mV s^{-1}. (b) Mass-normalized and (c) ESCA-normalized CV curves of various Pt_xRu-NCs in 1 M KOH + 0.1 M NH_3 solution at 50 mV s^{-1}. (d) AOR mass activity and specific activity of various Pt_xRu-NCs at 0.67 V.

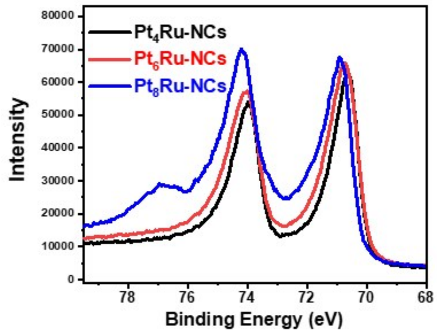

Fig. S8 Pt 4f XPS spectra of Pt_4Ru-NCs, Pt_6Ru-NCs and Pt_8Ru-NCs.

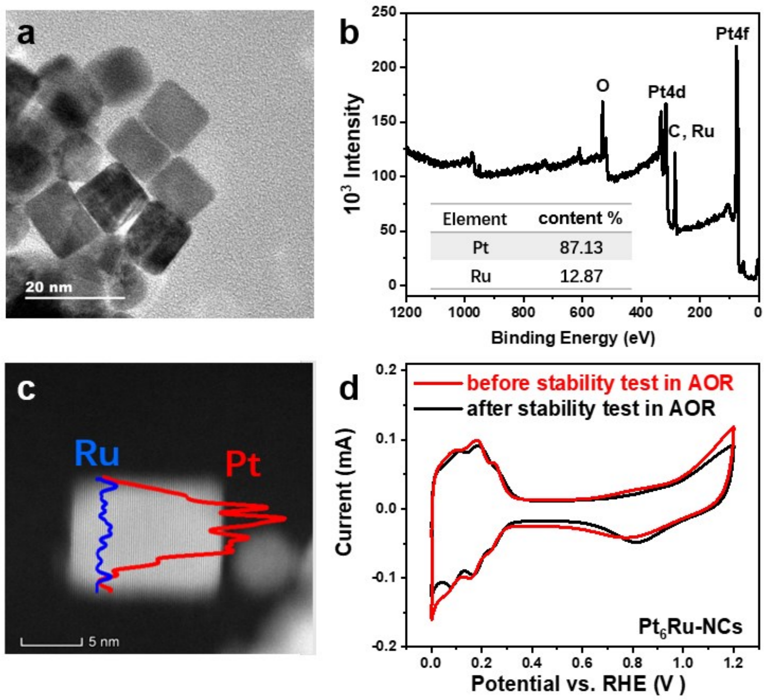

Fig. S9 (a) TEM image, (b) XPS spectrum of Pt_6Ru-NCs, (c) STEM EDX line scan spectrum and (d) CV curves of Pt_6Ru-NCs after the AOR stability test.

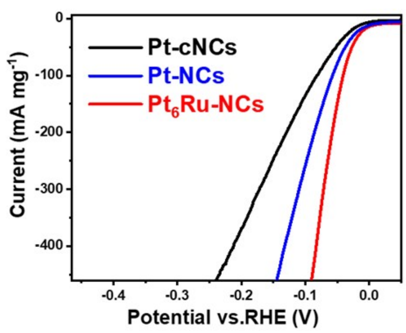

Fig. S10 HER polarization curves normalized by the total metal mass.

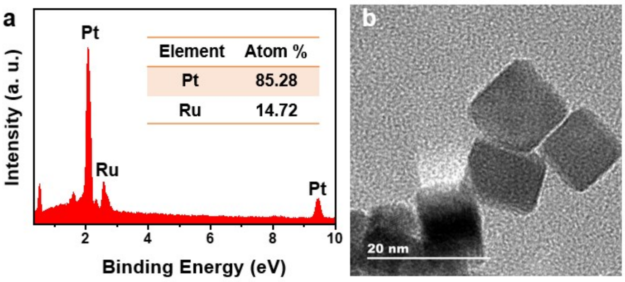

Fig. S11 (a) EDX spectrum and (b) TEM image of Pt_6Ru-NCs after the chronoamperometry tests.

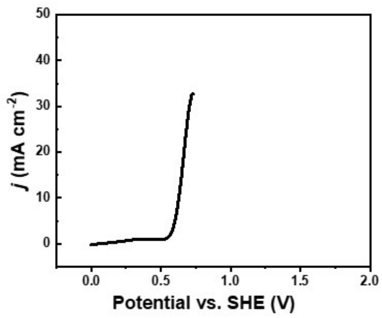

Fig. S12 Polarization curve of Pt_6Ru-NCs||Pt_6Ru-NCs electrolyzers (double loading) in 1 M KOH solution with 1 M NH_3 at 5 mV s^{-1}.

Table S1 The atomic ratio of Pt and Ru in Pt_xRu-NCs by ICP and XRD.

	Atomic ratio	**Pt_8Ru-NCs**	**Pt_6Ru-NCs**	**Pt_4Ru-NCs**
ICP	**Pt (%):Ru (%)**	89.05%:10.95%	85.76%:14.24%	80.33%:19.67%
XRD	**Pt (%):Ru (%)**	88.95%:11.05%	86.11%:13.89 %	80.15%:19.85%

Table S2 The peak potential or peak current of AOR at various Pt-based electrocatalysts in alkaline solution.

Catalysts	Electrolyte	C_{NH3} (M)	Scan rate mV s^{-1}	Peak potential (V vs. RHE)	Mass current (mA mg^{-1})	Specific current (mA cm^{-2})	Ref. (year)
Pt_6Ru-NCs	1 M KOH	0.1 M	50	0.67 V	192	1.02	This work
Pt-NCs	1 M KOH	0.1 M	5	0.66 V	135.25		2020[1]
Au@Pt NPs	1 M KOH	0.05 M	5	0.68 V		1.03	2020[2]

$PtIrNi_1/SiO_2$-CNT-COOH	1 M KOH	0.1 M	20	0.67 V	122		2020[3]
Pt_{ML} on Au	1 M KOH	0.1 M	50	0.7 V		0.27	2019[4]
Pt trigonal nano-pyramid	1 M KOH	1 M	10	0.7 V		0.4	2019[5]
annealed Pt[6] electrode	0.1 M KOH	1 mM	50	0.625 V		0.8	2019[7]
Cu–Pt	1 M KOH	0.1 M	2	-0.1 V vs Hg/HgO	2.5		2019[8]
Pt electrocatalysis	0.1 M KOH	1 mM	50	0.62 V		0.8	2018[9]
PtIr/C	1 M KOH	0.1 M	20	0.65 V	46		2018[10]
PtZn	0.5 M KOH	0.1 M	100	0.7 V		0.6	2017[11]
Pt/Rh	1 M NaOH	0.1 M	10	-0.3 V vs. Hg/HgO		0.55	2017[12]
Pt-Decorated Ni particles	1 M NaOH	0.1 M	10	0.7 V	75		2017[12]
Y_2O_3-modified Ptnanofilm	1 M KOH	0.1 M	20	0.65 V		0.18	2016[13]
Pt-NCs	1 M KOH	0.1 M	50	0.67 V	170		2016[14]
Pt-decorated flower-like	1 M KOH	0.1 M	10	0.69 V	75		2016[15]
Flower-like Pt particles consisting of Pt nanosheets	1 M KOH	0.1 M	10		46.8		2013[16]
Pt nanosheets	1 M KOH	0.1 M	10	−0.35 V(SCE)	70		2013[17]

Table S3 The η_{10} of HER on various Pt-based electrocatalysts in alkaline solution.

Catalysts	Electrolyte	Sweep rate	η_{10} value	Ref. (year)
Pt_6Ru-NCs	1 M KOH	5 mV s^{-1}	37.6 mV	This work
Pt-NCs	1 M KOH	10 mV s^{-1}	45 mV	2020[1]
Mo_2C@NC@Pt	1 M KOH	5 mV s^{-1}	47 mV	2019[18]
$Ni(OH)_2$ -Decorated Pt Nanocubes	0.1 M KOH	50 mV s^{-1}	69 mV	2019[19]
Co–Pt/C-10	1 M KOH	10 mV s^{-1}	50 mV	2018[20]

PtO_2–CoOOH/TM	1 M KOH	5 mV s^{-1}	40 mV	2018[21]
Pt–Ni branched nanocages	0.1 M KOH	10 mV s^{-1}	105 mV	2018[22]
NiCoN/C nanocages	1 M KOH		103 mV	2018[23]
$Ni_3[Fe(CN)_6]_2$/Pt	1 M KOH	2 mV s^{-1}	165 mV	2018[24]
PtNi–Ni NA/CC	0.1 M KOH	5 mV s^{-1}	51 mV	2018[25]
Pt/Ni@NGNTs	1 M KOH	10 mV s^{-1}	50 mV	2017[26]
Ni_3N/Pt nanosheets	1 M KOH	5 mV s^{-1}	50 mV	2017[27]
NiFe LDH-Pt-ht/CC	1 M KOH	5 mV s^{-1}	101 mV	2017[28]
Pd−Pt-S	1 M KOH	5 mV s^{-1}	70 mV	2017[29]
PtCo/C	0.1 M KOH	100 mV s^{-1}	50 mV	2017[30]

Notes and references

1 H.-Y. Sun, G.-R. Xu, F.-M. Li, Q.-L. Hong, P.-J. Jin, P. Chen and Y. Chen, *J. Energy Chem.*, 2020, **47**, 234-240.

2 J. Wang, J. Heo, C. Chen, A.J. Wilson and P.K. Jain, *Angew. Chem. Int. Ed. Engl.*, 2020, **59**, 1-6.

3 Y. Li, X. Li, H.S. Pillai, J. Lattimer, N.M. Adli, S. Karakalos, M. Chen, L. Guo, H. Xu, J. Yang, D. Su, H. Xin and G. Wu, *ACS Catal.*, 2020, **10**, 3945-3957.

4 J. Liu, B. Liu, Y. Wu, X. Chen, J. Zhang, Y. Deng, W. Hu and C. Zhong, *Catal.*, 2019, **9**.

5 S. Johnston, B.H.R. Suryanto and D.R. MacFarlane, *Electrochim. Acta*, 2019, **297**, 778-783.

6 E. Berlin, S. Garbarino, D. Guay, J. Solla-Gullon, F.J. Vidal-Iglesias and J.M. Feliu, *J. Power Sources*, 2013, **225**, 323-329.

7 H.S. Pillai and H. Xin, *Ind. Eng. Chem. Res.*, 2019, **58**, 10819-10828.

8 A.M. Pourrahimi, R.L. Andersson, K. Tjus, V. Strom, A. Bjork and R.T. Olsson, *Sustainable Energy Fuels*, 2019, **3**, 2111-2124.

9 I. Katsounaros, M.C. Figueiredo, F. Calle-Vallejo, H. Li, A.A. Gewirth, N.M. Markovic and M.T.M. Koper, *J. Catal.*, 2018, **359**, 82-91.

10 L. Song, Z. Liang, Z. Ma, Y. Zhang, J. Chen, R.R. Adzic and J.X. Wang, *J. Electrochem. Soc.*, 2018, **165**, J3095-J3100.

11 J. Jiang, *Electrochem. Commun.*, 2017, **75**, 52-55.

12 N.N. Fomena, S. Garbarino, E. Bertin, A. Korinek, G.A. Botton, L. Roue and D. Guay, *J. Catal.*, 2017, **354**, 270-277.

13 Y. Katayama, T. Okanishi, H. Muroyama, T. Matsui and K. Eguchi, *J. Catal.*, 2016, **344**, 496-506.

14 S. He, Z. Wu, S. Li and J.-M. Lee, *Int. J. Hydrogen Energy*, 2016, **41**, 1990-1996.

15 J. Liu, B. Chen, Y. Kou, Z. Liu, X. Chen, Y. Li, Y. Deng, X. Han, W. Hu and C. Zhong, *J. Mater. Chem. A*, 2016, **4**, 11060-11068.

16 J. Liu, W. Hu, C. Zhong and Y.F. Cheng, *J. Power Sources*, 2013, **223**, 165-174.

17 X.T. Du, Y. Yang, J. Liu, B. Liu, J.B. Liu, C. Zhong and W.B. Hu, *Electrochim. Acta*, 2013, **111**, 562-566.

18 J.-Q. Chi, J.-Y. Xie, W.-W. Zhang, B. Dong, J.-F. Qin, X.-Y. Zhang, J.-H. Lin, Y.-M. Chai and C.-G. Liu, *ACS Appl. Mater. Interfaces*, 2019, **11**, 4047-4056.

19 Y. Hong, C.H. Choi and S.-I. Choi, *ChemSusChem*, 2019, **12**, 4021-4028.

20 N. Meng, J. Ren, Y. Liu, Y. Huang, T. Petit and B. Zhang, *Energy Environ. Sci.*, 2018, **11**, 566-571.

21 Z. Wang, X. Ren, X. Shi, A.M. Asiri, L. Wang, X. Li, X. Sun, Q. Zhang and H. Wang, *J. Mater. Chem. A*, 2018, **6**, 3864-3868.

22 Z. Cao, H. Li, C. Zhan, J. Zhang, W. Wang, B. Xu, F. Lu, Y. Jiang, Z. Xie and L. Zheng, *Nanoscale*, 2018, **10**, 5072-5077.

23 J. Lai, B. Huang, Y. Chao, X. Chen and S. Guo, *Adv. Mater.*, 2019, **31**, 1805541.

24 X. Zhang, P. Liu, Y. Sun, T. Zhan, Q. Liu, L. Tang, J. Guo and Y. Xia, *Inorg. Chem. Front.*, 2018, **5**, 1683-1689.

25 L. Xie, Q. Liu, X. Shi, A.M. Asiri, Y. Luo and X. Sun, *Inorg. Chem. Front.*, 2018, **5**, 1365-1369.

26 X. Bao, J. Wang, X. Lian, H. Jin, S. Wang and Y. Wang, *J. Mater. Chem. A*, 2017, **5**, 16249–16254.

27 Y. Wang, L. Chen, X. Yu, Y. Wang and G. Zheng, *Adv. Energy Mater.*, 2017, **7**, 1601390.

28 S. Anantharaj, K. Karthick, M. Venkatesh, T.V.S.V. Simha, A.S. Salunke, L. Ma, H. Liang and S. Kundu, *Nano Energy*, 2017, **39**, 30-43.

29 J. Fan, K. Qi, L. Zhang, H. Zhang, S. Yu and X. Cui, *ACS Appl. Mater. Interfaces*, 2017, **9**, 18008-18014.

30 Q. Chen, Z. Cao, G. Du, Q. Kuang, J. Huang, Z. Xie and L. Zheng, *Nano Energy*, 2017, **39**, 582-589.